Distributed Event-triggered Bipartite Consensus for Model-free MASs Against Injection Attacks

Huarong Zhao[1,2], Jinjun Shan[2], Li Peng[1], Hongnian Yu[3]

1. Research Center of Engineering Applications for IoT, Jiangnan University, Wuxi 214122, China

E-mail: zhaohuarong@stu.jiangnan.edu.cn

2. Department of Earth and Space Science and Engineering, York University, 4700 Keele Street, Toronto, M3J1P3, Canada
E-mail: jjshan@yorku.ca

3. School of Engineering and the Built Environment, Edinburgh Napier University, EH10 5DT Edinburgh, UK
E-mail: h.yu@napier.ac.uk

Abstract: This paper studies fully distributed data-driven problems for heterogeneous nonlinear discrete-time multiagent systems (MASs) with fixed and switching topologies preventing injection attacks. We first develop an enhanced compact form dynamic linearization model by applying the designed distributed bipartite combined measurement error function of the MASs,. we then an event-triggered control machination is developed and, a fully distributed event-triggered bipartite consensus framework is designed, where the dynamics information of MASs is no longer needed. Meanwhile, the restriction of topology is further relieved, which is fitting leader-less, leader-follower, and even containment control. Moreover, to prevent injection attacks, nervous network-based detection and compensation schemes are developed. Rigorous convergence proof is presented that the bipartite consensus error is ultimately boundedness by utilizing the Lyapunov stability theory. Finally, the correctness and effectiveness of the designed method are verified by simulation and hardware experiments.

Key Words: Multiagent systems, bipartite consensus, data-driven control, injection attacks, neural network.

I. Introduction

In recent decades, collaborative control of multi-agent systems (MASs) has been a vital investigation field, and numerous excellent results for formation or consensus control are developed because of the wide application scenarios, such as the formation of unmanned aerial vehicles, rendezvous of space shuttles, and cooperative handling of multi-manipulators [1-2]. The consensus control is to formulate an appropriate distributed control protocol for a group of agents to reach a consistent state. There are two major categories of MASs, leader-less consensus [3-4] and leader-follower consensus [5-6].

Most distributed results [1-6] need the local information of agents and the global connectivity information of the communication graph to develop an appropriate control protocol, especially the knowledge of the smallest nonzero eigenvalue of the Laplacian matrix of the graph. To relieve the restrictions of the graph, a fully distributed concept, which only requires the graph containing a directed spanning tree, is proposed. As for linear MASs, Movric et al. [7] and Li et al. [8] proposed the distributed cooperative optimal control protocol and the fully distributed consensus (FDC) protocol, respectively. Lv et al. [9] further demonstrated the sufficient and necessary condition of linear MASs to realize FDC control. Second-order and high-order MASs were investigated by Wang et al. [10] and Zhang et al. [11]. It should be pointed out that previous effects of FDC are only focused on linear MASs, while the research of FDC for nonlinear MASs is at the early stage.

Obtaining accurate dynamics of the controlled nonlinear plant is a huge challenge of most existing model-based control (MBC) protocols [3-11], especially for large-scale heterogeneous nonlinear MASs. therefore, an alternative method has been developed recently, called data-driven control (DDC) or model-free control. Roughly speaking, DDC can be categorized into DDC with neural networks (NNs) and DDC without NNs. Reinforcement learning [12-13] is a classic DDC with actor-critic NNs and has excellent control performance for governing the complex MASs. However, the training process is a significant effort, where the training data and test data must be sufficiently available from the different operating environments. The model-free adaptive control framework for a single nonlinear system was first proposed by Hou et al. [14]. Their method only depends on the input and output data to online update a parameter of the controller without establishing NNs. Moreover, event-triggered control [15-16], fault-tolerant control [17-18], and resilient control [19-20] are also investigated.

However, the existing methods [14-20] only consider a single system. As for MASs, few effects have been made, such as Bu et al. [21] extended MFAC for MASs, Xiong et al. [22] studied the sensor fault issue, and Ma et al. [23] investigated the denial-of-service (DoS) attacks issue. MASs is more complicated than a single system, so further studying a novel DDC framework for unknown nonlinear MASs is more meaningful and challenging work than a singlesystem.

In practical systems, the information transaction among MASs usually depends on a publicly shared communication network. Hence, effectively utilizing the limited network batch and preventing cyberattacks is a meaningful topic. Event-triggered control (ETC) was first

*This work is supported by National Natural Science Foundation (NNSF) of China under Grant 00000000.

developed by Dimarogonas et al. [24], a reliable scheme for saving the communication resources for the MASs with acceptable performance. The fully distributed ETC schemes for linear and nonlinear MASs were investigated by Zhang et al. [25] and Sun et al. [26], respectively. In addition, for the network security issues, DoS attacks [27], deception attacks [28], and false data injection attacks [29] are usually considered for MASs, where the data injection attack (DIA) is extensively studied. Li et al. [29] designed an ETC for discrete time-varying MASs with DIA. Ahmed et al. [30] proposed a frequency domain analysis method for MASs against DIA. Dong et al. [31] developed a resilient consensus method for MASs under external and malicious DIA. However, from the motivated literature, it is found that few DDC efforts are made for addressing the resource utilization and DIA issues together.

Moreover, collaborative and antagonistic relationships are coexistence. The results above have a common assumption that the relationship among agents is cooperative. As for the issue of the antagonistic interaction, it was first studied by Altafini [32], where the concept of bipartite consensus (BC) and signed networks are given. BC aims to realize a tracking task with a couple of opposite objectives for two groups of agents, such as two teams in a game. Chen et al. [33] studied a BC method for MASs employing partial differential equations. Sakthivel et al. [34] proposed a dynamic output feedback control method for MASs to conduct bipartite consensus tasks. Moreover, a data-driven bipartite consensus method was designed by Peng et al. [35].

Following the above discussions and motivation, we study a class of unknown nonlinear nonaffine discrete-time MASs and address the issues of antagonistic interactions, data injection attacks, and limited communication bandwidth. The main contributions of this paper are summarized below.

(1) Establish an enhanced compact form dynamic linearization model. Comparing with CFDL in [14], we consider the information of the agent's neighbors and the antagonistic interactions among agents.

(2) Formulate a fully distributed event-triggered bipartite consensus (DETBC) framework without the requirement of the dynamics information andglobal connectivity information of the nonlinear MASs. Comparing with the previous DDC methods [19-23], we not only improve the convergence rate, but also reduce communication resources.

(3) Design NNs-based attack detection and compensation schemes. Comparing with existing NNs-based algorithms [16-17], our schemes have stronger detection capability without the requirement of the training and testing data.

(4) Rigorously prove the convergence of the proposed schemes which are also experimentally verified. We also presented the sufficient and necessary conditions of the proposed schemes.

The rest of this paper includes the following sections. Section II presents the basic knowledge of signal graph theory and the characteristic of controlled MASs. The DETBC method is designed and analyzed in Section III. Section IV and V give the summation and hardware tests, respectively. Section VI presents several summarizations.

Notations: R, R^+, R^N, $R^{N\times N}$, Z^+, and I, denote the set of real numbers, positive real numbers, N dimensions column vectors, N dimensions square matrices, positive integers, and identify matrices with arbitrary dimension, respectively. $diag(\bullet)$, $sign(\bullet)$, and $round(\bullet)$ stand for diagonal matrix, sign function, and rounding function, respectively. $\|\Theta\|$ represents the Euclidean norm of the vector $\Theta\in R^N$. Moreover, k=1,2,… represents the time interval.

II. Preliminary and Problem Formulation

A. Signed Graph Theory

This article employs a signed graph $G=(V,E,A)$ to describe the communication topology of the MASs with N agents, where $V=\{1,\cdots,N\}$, $E=\{(i,j)\,|\,i,j\in V, i\neq j\}\subseteq V\times V$, and $A=[a_{ij}]\in R^{N\times N}$ represent nodes, edges, and the weighted adjacency matrix with elements -1, 0, 1, respectively, $N_i=\{j\in V\,|\,(j,i)\in E\}$ stands for the neighborhood set of the node i, and $D=diag\{d_1,\cdots,d_N\}$ with $d_i=\sum_{j\in N_i}|a_{ij}|$ stands for the degree matrix of G. Define an augmentation graph as $\bar{G}=(\bar{V},\bar{E},A)$ with $\bar{V}=V\bigcup\{0\}$ and $\bar{E}=\bar{V}\times\bar{V}$, where node 0 represents the virtual leader. $L=-A+D$ is the Laplacian matrix of $\bar{G}$. Let matrix $B=diag\{b_1,\cdots,b_N\}$ expresse how the information is transmitted from the virtual leader to followers, where if the agent i directly receives the data from the virtual leader, $b_i=1$; otherwise $b_i=0$.

Moreover, $\bar{G}$ is structurally balanced and includes two opposite groups U_1 and U_2. The main characteristics of the two groups are concluded as : 1) $U_1\bigcup U_2=V$ and $U_1\bigcap U_2=\varnothing$; 2) If $\forall i,j\in U_l$ with $l\in\{1,2\}$, $a_{ij}\in\{0,1\}$; 3) If $\forall i\in V_l$ and $j\in U_p$ with $p\in\{1,2\}$ and $l\neq p$, $a_{ij}\in\{-1,0\}$. If $(i,j)\notin E$ or $i=j$, $a_{ij}=0$. The relationship between agents and groups is denoted by grouping matrix $s=diag(s_1,\cdots,s_N)$ with $s_i\in\{1,-1\}$, where $s_i=1$ denotes the agent i belongs to U_1; otherwise the agent i belongs to U_2. In addition, the set of agents is denoted by A_N.

Lemma 1: If the graph $\bar{G}$ has a directed spanning tree, the matrix $\hat{L}$=L+B is positive definite.

B. System Description

A class of SISO (single-input-single-output) nonlinear nonaffine discrete-time MASs with N agents is investigated, and the input and output of the *ith* agent satisfy:

$$y_i(k+1)=p_i(y_i(k),u_i(k)), \tag{1}$$

where $u_i(k)\in R$ and $y_i(k)\in R$ represent the input and output of agent i with $i\in A_N$, respectively. Moreover, $u_i(k)$ and $y_i(k)$ are bounded by r_u and r_y, respectively. $p_i(\bullet)$ is an unknown nonlinear function, and the communication topology of MASs is denoted by $\bar{G}$.

The basic restrict conditions of Eq. (1) are given below.

***Assumption 1*:** The value $\partial p_i^*/\partial u_i(k)$ is continuous.

***Assumption 2*:** The generalized Lipschitz condition can be applied for Eq. (1), where if $\Delta u_i(k)\neq 0$, there is a constant r satisfying $|\Delta y_i(k+1)|\leq r|\Delta u_i(k)|$ for all k, where $\Delta u_i(k)=u_i(k)-u_i(k-1)$ and $\Delta y_i(k)=y_i(k)-y_i(k-1)$.

Remark 1: Assumptions 1 and 2 are reasonable and are usually used in model-based control theory. In this paper, the input and output data are utilized to realize online learning, so they are must be bounded. Moreover, according to energy conservation, the output energy should not be infinite if the input energy is limited.

To analysis fully distributed bipartite consensus issues, the following assumption is used.

***Assumption 3*:** The value of $|\Delta u_j(k)/\Delta u_i(k)|$ exists and is bounded by r_Δ, which is a constant, where $\Delta u_j(k)$ is the input gain of agent *i*'s neighbors.

Generally, the distributed BC combined measurement error of MASs is designed as

$$\begin{aligned}\zeta_i(k+1)=&\sum_{j\in N_i}|a_{ij}|(sign(a_{ij})y_i(k+1)-y_j(k+1))\\&+b_i(s_iy_0(k+1)-y_i(k+1))\end{aligned}\tag{2}$$

where $y_j(k)$ is the output of agent *i*'s neighbors, $y_0(k)$ is output of the leader bounded by r_0, a_{ij}, b_i, and s_i are defined in Section II.A. From Eq. (1), we have

$$\begin{aligned}\zeta_i(k+1)=&\sum_{j\in N_i}|a_{ij}|(sign(a_{ij})p_i(y_i(k),u_i(k))-p_j(y_j(k),u_j(k)))\\&+b_i(s_iy_0(k+1)-p_i(y_i(k),u_i(k)))\end{aligned}\tag{3}$$

From Eq. (3), it is found that $\zeta_i(k+1)$ consists of nonlinear functions $p_i(y_i(k),u_i(k))$ and $p_j(y_j(k),u_j(k))$. Hence, define a new nonlinear function $P_i(y_i(k),u_i(k),y_j(k),u_j(k))$. Thus, according to the similar analysis in [14], we have

$$\zeta_i(k+1)=P_i(y_i(k),u_i(k),y_j(k),u_j(k)),\ j\in N_i\tag{4}$$

and obtain the following Theorem.

***Theorem 1*:** Considering that the input and output data of MASs satisfy Assumptions 1-4 and Eq. (4), an enhanced compact form dynamic linearization (E-CFDL) model of the MASs is formulated as

$$\Delta\zeta_i(k+1)=\Gamma_i(k)\Delta u_i(k),\tag{5}$$

where $\Delta\zeta_i(k+1)=\zeta_i(k+1)-\zeta_i(k)$, and $\Gamma_i(k)$ is a time-varying pseudo-partial-derivative (PPD) parameter and bounded by a constant $r_\zeta\in R^+$.

Proof: See Appendix A.

Remark 2: The designed E-CFDL has similar characteristics to the existing CFDL in [14] and [21]. However, the CFDL in [14] and [21] merely considers the input and output of a single agent. From Eqs. (3) and (4), it is found that the proposed E-CFDL employs the input and output information of agent *i* and its neighbors. Hence, the proposed E-CFDL is more applicable to analyze MASs.

***Assumption 4*:** For Eq. (5), the learning direction is dependent on $\Gamma_i(k)>0$ or $\Gamma_i(k)<0$. According to the analysis of the existing CFDL, the PPD parameter of the designed E-CFDL also is assumed as positive.

***Assumption 5*:** The graph $\bar{G}$ has a directed spanning tree.

C. Injection Attack Description

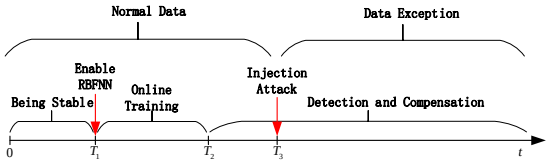

Fig. 1: The operation process of the designed DETBC method

Generally speaking, machines are running nominal satisfying Eq. (1) at the beginning when the factory buys them. However, if the machine is subject to cyber-attack or physical-attack, the following equation is considered

$$y_{si}(k)=y_i(k)+f_{si}(k)\tag{6}$$

where $f_{si}(k)$ is the unknown injected data, $y_i(k)$ is the actual output of a machine, and $y_{si}(k)$ is the sampled data of the machine.

Assumptions 6: $f_{si}(k)$ is bounded by a constant r_{ys}.

Figure 1 shows the E-CFDL model of MASs presented in Eq. (5) during the normal data process. If the injection attack is successfully at $k=T_3$, the function of the E-CFDL model is changed because the output of MASs becomes $y_{si}(k)$. Then, using the similar analysis of Section II.B, we obtain the corresponding E-CFDL

$$\Delta\zeta_{si}(k+1)=\Gamma_{si}(k)\Delta u_i(k)\tag{7}$$

where $\Delta\zeta_{si}(k+1)=\zeta_{si}(k+1)-\zeta_{si}(k)$, $\Gamma_{si}(k)$ is bounded by a constant $r_{\zeta s}$, and

$$\begin{aligned}\zeta_{si}(k+1)=&\sum_{j\in N_i}|a_{ij}|(sign(a_{ij})y_{si}(k+1)-y_{sj}(k+1))\\&+b_i(s_iy_0(k+1)-y_{si}(k+1))\end{aligned}\tag{8}$$

Definition1: The bipartite consensus error $e_i(k)=s_iy_0(k)-y_i(k)$ with $i\in A_N$ is bounded when k towards infinity, whatever the output data is normal or exception as shown in Fig.1.

Remark 3: It is noteworthy that this paper aims to formulate a fully distributed event-triggered bipartite consensus (DETBC) framework and develop an active attack detection and prevention approach using the radial basis function neural network (RBFNN).

III. DETBC Algorithm Development and Analysis

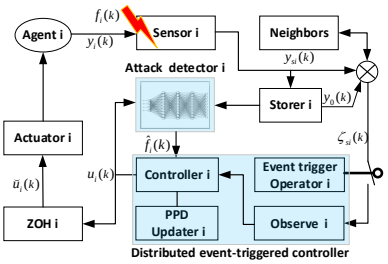

Fig. 2: The diagram of the developed DETBC approach

Figure 2 shows tThe proposed DETBC scheme whichconsists of an event-triggered (ET) operator, distributed BC combined measurement error observer, RBFNN-based attack detector, storer, and zero-order hold (ZOH). If the ET operator doesn't turn on the switch, the ZOH will not update the output, that is, $\bar{u}_i(k)=u_i(k_i)$, where k_i denotes the last ET instant and $k_i\leq k<k_{i+1}$. Figure 1 illustrates the operation process of the designed DETBC

method, which includes three steps, being stable, online training, and detection and compensation. Step 1: employ the designed DETBC to realize event-triggered bipartite consensus control for MASs with injection attack-free. Step 2: train the parameters of RBFNN using the input and output data of the MASs to ensure the RBFNN can predict the output of the MASs with injection attack-free. Step 3: the proposed DETBC employs the predicted results to detect the attack and reduce the effects.

A. RBFNN-based Attack Detection and Compensation

In this study, RBFNN is employed to learn the characteristics and predict the output of the MASs with injection attack-free. The input vector is set as $X_i=[u_i(k), u_i(k-1), y_0(k), y_0(k-1)]^T$, and the radial basis vector is defined as $\boldsymbol{\phi}_i(\bullet)=[\boldsymbol{\phi}_{i1}(\bullet),\boldsymbol{\phi}_{i2}(\bullet),\cdots,\boldsymbol{\phi}_{in}(\bullet)]^T$, where n denotes the number of nervous in the hidden layer, which is obtained based on the practical applications. Using Gauss basis function as the radial basis function is expressed as

$$\boldsymbol{\phi}_{il}(X_i(k))=\exp(-\| X_i(k)-m_i \| /(2\boldsymbol{\sigma}_i^2)),\ l=1,2,...,n \quad (9)$$

where m_i and $\boldsymbol{\sigma}_i$ are center vector and basis width vector, respectively. Applying the universal approximation theorem [36], the RBFNN can obtain an appropriate weight vector $\hat{\mathrm{W}}_i(k)=[\hat{w}_1(k),\hat{w}_2(k),\cdots,\hat{w}_n(k)]^T$, that is, there is an acceptable constant $\hbar$ satisfying $|y_i(k)-\hat{y}_i(k)|\leq\hbar$, where $\hat{y}_i(k)=\hat{\mathrm{W}}_i(k)\boldsymbol{\phi}_i(X_i(k))$, and index function is defined as $J=1/2\sum_k(y_i(k)-\hat{y}_i(k))^2$. The details about RBFNN can be found in [36] and [37].

Hence, according to $\hat{y}_i(k)$, an injection attack detection scheme is designed as

$$\hat{f}_i(k)=y_{si}(k)-\hat{y}_i(k), \quad (10)$$

If $|\hat{f}_i(k)|>\hbar$, the agent i is subject to an injection attack and the injected data is $\hat{f}_i(k)$, where $\hbar$ is often determined by experiments or experiences of experts.

To compensation the effects of injection attack, we design a compensation scheme is designed based on Eq. (8) as below

$$\begin{aligned}\zeta_{si}(k)=&\sum_{j\in N_i}|a_{ij}|(sign(a_{ij})y_{si}(k)-y_{sj}(k))\\&+b_i(s_iy_0(k)-y_{si}(k)+\hat{f}_i(k))\end{aligned} \quad (11)$$

Remark 3: The established NNs are employed to identify the dynamics of controlled systems running normally. Hence, the established NNs can recognize all of the differences caused by cyberattacks or physical corruption. However, most existing methods [16][17] only can address issues, which have been considered in the training process.

B. Event-based PPD Parameter Estimator

Case 1: $0<k<T_3$, without injection attack. In this case, the event-triggered PPD parameter estimator is designed as

$$\hat{\Gamma}_i(k)=\begin{cases}\hat{\Gamma}_i(k-1)+h\Delta u_i(k-1)/(\Delta u_i^2(k-1)+\theta)\\ \times(\Delta\zeta_i(k)-\hat{\Gamma}_i(k-1)\Delta u_i(k-1)), & k=k_i\\ \hat{\Gamma}_i(k_i), & k_i<k<k_{i+1}\end{cases} \quad (12)$$

where $0<h<1$ and $\theta>0$. To improve the estimation performance of Eq. (12), a reset law is designed as

$$\hat{\Gamma}_i(k)=\hat{\Gamma}_i(1), \quad \text{if } |\Delta\hat{\Gamma}_i(k)|\leq\delta \text{ or } |\Delta u_i(k-1)|\leq\delta \text{ or } \operatorname{sign}(\hat{\Gamma}_i(k))\neq\operatorname{sign}(\hat{\Gamma}_i(1)) \quad (13)$$

where δ is often set as 10^{-4} of 10^{-5}.

Theorem 2: Using the PPD parameter updated by Eqs. (12)-(13), with $\tilde{\Gamma}_i(k)=\hat{\Gamma}_i(k)-\Gamma_i(k)$ can achieve that $\tilde{\Gamma}_i(k)$ and $\hat{\Gamma}_i(k)$ are bounded by $\hat{r}\in R^+$ and $\tilde{r}\in R^+$, respectively.

Proof: To achieve the boundedness of $\tilde{\Gamma}_i(k)$ and $\hat{\Gamma}_i(k)$, the following two different situations should be discussed.

Case 1.1: $k=k_i$, the event is triggered. From Eq. (12) and $\tilde{\Gamma}_i(k)=\hat{\Gamma}_i(k)-\Gamma_i(k)$, we obtain the following equation

$$\begin{aligned}\tilde{\Gamma}_i(k)=&\tilde{\Gamma}_i(k-1)-\Gamma_i(k)+\Gamma_i(k-1)\\&-h\tilde{\Gamma}_i(k-1)\Delta u_i^2(k-1)/(\Delta u_i^2(k-1)+\theta)\\=&(1-h\Delta u_i^2(k-1)/(\Delta u_i^2(k-1)+\theta))\tilde{\Gamma}_i(k-1)\\&-\Gamma_i(k)+\Gamma_i(k-1)\end{aligned} \quad (14)$$

Since $0<h<1$ and $\theta>0$, there is a constant q_1 satisfying $0<|(1-h\Delta u_i^2(k-1)/(\Delta u_i^2(k-1)+\theta))|<q_1<1$. Thus, we have

$$\begin{aligned}|\tilde{\Gamma}_i(k)|&\leq q_1|\tilde{\Gamma}_i(k-1)|+|2\Gamma_i(k-1)|\\&\leq q_1|\tilde{\Gamma}_i(k-1)|+2r_\zeta\\&\cdots\\&\leq q_1^{k-1}|\tilde{\Gamma}_i(1)|+2r_\zeta(1-q_1^{k-1})/(1-q_1)\end{aligned} \quad (15)$$

Hence, $\lim_{k\to\infty}|\tilde{\Gamma}_i(k)|\leq\tilde{r}$ with $\tilde{r}=2r_\zeta/(1-q_1)$. Since $\tilde{\Gamma}_i(k)=\hat{\Gamma}_i(k)-\Gamma_i(k)$ and $|\Gamma_i(k)|\leq r_\zeta$, there is a constant $\hat{r}$ satisfying $|\hat{\Gamma}_i(k)|\leq\hat{r}$.

Case 1.2: $k_i<k<k_{i+1}$, event is not triggered. From Eq. (12), we have $\hat{\Gamma}_i(k)=\hat{\Gamma}_i(k_i)$. According to $|\hat{\Gamma}_i(k_i)|<\hat{r}$ and the analysis of Case 1.1 in Theorem 1, it is obtained that $\tilde{\Gamma}_i(k)$ and $\hat{\Gamma}_i(k)$ are bounded. □

Case 2: $T_3\leq k$, with injection attack. We design the corresponding PPD parameter estimator as

$$\hat{\Gamma}_{si}(k)=\begin{cases}\hat{\Gamma}_{si}(k-1)+h\Delta u_i(k-1)/(\Delta u_i^2(k-1)+\theta)\\ \times(\Delta\zeta_{si}(k)-\hat{\Gamma}_{si}(k-1)\Delta u_i(k-1)), & k=k_i\\ \hat{\Gamma}_{si}(k_i), & k_i<k<k_{i+1}\end{cases}, \quad (16)$$

where $0<h<1$, $\theta>0$, and propose a reset law as

$$\hat{\Gamma}_{si}(k)=\hat{\Gamma}_{si}(1), \quad \text{if } |\Delta\hat{\Gamma}_{si}(k)|\leq\delta \text{ or } |\Delta u_i(k-1)|\leq\delta \text{ or } \operatorname{sign}(\hat{\Gamma}_{si}(k))\neq\operatorname{sign}(\hat{\Gamma}_{si}(1)) \quad (17)$$

where δ is often set as 10^{-4} of 10^{-5}.

Thus, according to the analysis of Theorem 1, we obtain those constants $\hat{r}_s$ and $\tilde{r}_s$ which satisfy $|\hat{\Gamma}_{si}(k)|\leq\hat{r}_s$ and $|\tilde{\Gamma}_{si}(k)|\leq\tilde{r}_s$, respectively.

C. Observer-based Event-triggered Mechanism

An observer of the BC combined measurement error is designed as

$$\hat{\zeta}_i(k+1)=\hat{\zeta}_i(k)+\hat{\Gamma}_i(k)\Delta\breve{u}_i(k)+x(\breve{\zeta}_i(k)-\hat{\zeta}_i(k)),\ 0<k<T_3 \quad (18)$$

$$\hat{\zeta}_{si}(k+1)=\hat{\zeta}_{si}(k)+\hat{\Gamma}_{si}(k)\Delta\breve{u}_i(k)+x(\breve{\zeta}_{si}(k)-\hat{\zeta}_{si}(k)),\ T_3\leq k \quad (19)$$

where x is the feedback gain, $\breve{\zeta}_i(k)=\zeta_i(k_i)$, $\breve{\zeta}_{si}(k)=\zeta_{si}(k_i)$, and $\Delta\breve{u}_i(k)=\Delta u_i(k_i)$, $k_i\leq k<k_{i+1}$. Moreover, $\zeta_i(k)$ and

$\zeta_{si}(k)$ are defined in Eqs. (3) and (11), respectively. Let $e_{\zeta i}(k)=\zeta_i(k)-\hat{\zeta}_i(k)$ and $e_{\zeta si}(k)=\zeta_{si}(k)-\hat{\zeta}_{si}(k)$ denote the observer error of $\zeta_i(k)$ and $\zeta_{si}(k)$, respectively. The ET incremental input error is defined as

$$\varepsilon_i(k)=\Delta u_i(k)-\Delta\breve{u}_i(k),\ 0<k<T_3, \tag{20}$$

$$\varepsilon_{si}(k)=\Delta u_i(k)-\Delta\breve{u}_i(k),\ T_3\le k, \tag{21}$$

Thus, the ET condition is obtained as

$$D(|\varepsilon_i(k)|)>E|e_{\zeta i}(k)|,\ 0<k<T_3, \tag{22}$$

$$D(|\varepsilon_{si}(k)|)>E_s|e_{\zeta si}(k)|,\ T_3\le k, \tag{23}$$

where $0<u<1$, $E=\sqrt{u(1-4(1-x)^2)/(4\hat{r}^2)}$, x is presented later on, and $E_s=\sqrt{u(1-4(1-x)^2)/(4\hat{r}_s^2)}$. Then, a dead-zone operator is defined as

$$D(|\varepsilon_i(k)|)=\begin{cases}|\varepsilon_i(k)|, & |e_{\zeta i}(k)|>\tau\\ 0, & otherwise\end{cases},\ 0<k<T_3, \tag{24}$$

$$D(|\varepsilon_{si}(k)|)=\begin{cases}|\varepsilon_{si}(k)|, & |e_{\zeta si}(k)|>\tau\\ 0, & otherwise\end{cases},\ T_3\le k, \tag{25}$$

where τ is discussed later on.

Theorem 3: Supposing that system (1) satisfies Assumptions 1-4 andobeys the corresponding conditions as Eqs. (23) and (24), and the injected data is restricted by Assumption 6, the corresponding observers designed in Eqs. (20) and (21) are bounded.

Proof : **Case 1:** $0<k<T_3$, during the normal data process. Using $e_{\zeta i}(k)=\zeta_i(k)-\hat{\zeta}_i(k)$, we have

$$\begin{aligned}e_{\zeta i}(k+1)&=\zeta_i(k+1)-\hat{\zeta}_i(k)-\hat{\Gamma}_i(k)\Delta\breve{u}_i(k)-x(\breve{\zeta}_i(k)-\hat{\zeta}_i(k))\\&=\zeta_i(k)+\Gamma_i(k)\Delta u_i(k)-\hat{\zeta}_i(k)-\hat{\Gamma}_i(k)\Delta\breve{u}_i(k)\\&\quad-x(\breve{\zeta}_i(k)-\hat{\zeta}_i(k))\\&=e_{\zeta i}(k)+\Gamma_i(k)\Delta u_i(k)-\hat{\Gamma}_i(k)\Delta u_i(k)\\&\quad+\hat{\Gamma}_i(k)\Delta u_i(k)-\hat{\Gamma}_i(k)\Delta\breve{u}_i(k)-x(\breve{\zeta}_i(k)-\hat{\zeta}_i(k))\\&=e_{\zeta i}(k)-\tilde{\Gamma}_i(k)\Delta u_i(k)+\hat{\Gamma}_i(k)\varepsilon_i(k)-x\breve{\zeta}_i(k)\\&\quad+x\hat{\zeta}_i(k)-x\zeta_i(k)+x\zeta_i(k)\\&=(1-x)e_{\zeta i}(k)-\tilde{\Gamma}_i(k)\Delta u_i(k)+\hat{\Gamma}_i(k)\varepsilon_i(k)\\&\quad+x(\zeta_i(k)-\breve{\zeta}_i(k))\end{aligned} \tag{26}$$

Define a Lyapunov function as $V_i(k)=e_{\zeta i}(k)$.

Case 1.1: $k=k_i$, the event is triggered. In this case, $\breve{\zeta}_i(k)=\zeta_i(k)$ and $\Delta\breve{u}_i(k)=\Delta u_i(k)$, we have

$$\begin{aligned}\Delta V_i(k+1)&=e_{\zeta i}^2(k+1)-e_{\zeta i}^2(k)\\&=((1-x)e_{\zeta i}(k)-\tilde{\Gamma}_i(k)\Delta u_i(k))^2-e_{\zeta i}^2(k)\\&\le 2(1-x)^2e_{\zeta i}^2(k)+2\tilde{\Gamma}_i^2(k)\Delta u_i^2(k)-e_{\zeta i}^2(k)\\&\le-(1-2(1-x)^2)e_{\zeta i}^2(k)+\Omega\end{aligned} \tag{27}$$

where $\Omega\ge 2\tilde{r}^2r_u^2\ge 2\tilde{\Gamma}_i^2(k)\Delta u_i^2(k)$.

Let $-(1-2(1-x)^2)e_{\zeta i}^2(k)+\Omega<0$, that is, $\Delta V_i(k+1)<0$, and

$$|e_{\zeta i}(k)|>\sqrt{\Omega/(1-2(1-x)^2)}=\tau, \tag{28}$$

where $(2-\sqrt{2})/2<x<(2+\sqrt{2})/2$.

Case 1.2: $k_i<k<k_{i+1}$, the event is not triggered. In this case, Eq. (27) is rewritten as

$$\begin{aligned}\Delta V_i(k+1)&=((1-x)e_{\zeta i}(k)+x(\zeta_i(k)-\zeta_i(k_i))-\tilde{\Gamma}_i(k)\Delta u_i(k)\\&\quad+\hat{\Gamma}_i(k)\varepsilon_i(k))^2-e_{\zeta i}^2(k)\\&\le 4(1-x)^2e_{\zeta i}^2(k)+4x^2(\zeta_i(k)-\zeta_i(k_i))^2\\&\quad+4\tilde{\Gamma}_i^2(k)\Delta u_i^2(k)+4\hat{\Gamma}_i^2(k)\varepsilon_i^2(k)-e_{\zeta i}^2(k)\\&\le-(1-4(1-x)^2)e_{\zeta i}^2(k)+4\hat{r}^2\varepsilon_i^2(k)+\Theta\end{aligned} \tag{29}$$

where $\Theta\ge 4x^2(\zeta_i(k)-\zeta_i(k_i))^2+4\tilde{\Gamma}_i^2(k)\Delta u_i^2(k)$ is bounded since $\Delta\zeta_i(k)$, $\tilde{\Gamma}_i(k)$ and $\Delta u_i^2(k)$ are bounded discussed previously. According to Eq. (22) and $k_i<k<k_{i+1}$,

$$4\hat{r}^2\varepsilon_i^2(k)\le u(1-4(1-x)^2)e_{\zeta i}^2(k), \tag{30}$$

Thus, Eq. (29) becomes

$$\begin{aligned}\Delta V_i(k+1)&\le-(1-4(1-x)^2)e_{\zeta i}^2(k)+u(1-4(1-x)^2)e_{\zeta i}^2(k)+\Theta\\&\le-(1-u(1-4(1-x)^2))e_{\zeta i}^2(k)+\Theta\\&\le-(1-u(1-4(1-x)^2))V_i(k)+\Theta\end{aligned} \tag{31}$$

and

$$\begin{aligned}V_i(k+1)&\le(1-(1-u(1-4(1-x)^2)))V_i(k)+\Theta\\&\cdots\\&\le(1-(1-u(1-4(1-x)^2)))^kV_i(1)\\&\quad+\Theta\frac{1-(1-(1-u(1-4(1-x)^2)))^k}{1-(1-(1-u(1-4(1-x)^2)))}\end{aligned} \tag{32}$$

Since $0<(1-u(1-4(1-x)^2))<1$ and $1/2<x<3/2$, $V_i(k+1)$ is bounded, that is, $e_{\zeta i}(k)$ is bounded.

Case 2: $T_3\le k$, during the data exception. According to the similar analysis of Case 1, we also obtain that $e_{\zeta si}(k)$ is bounded. □

D. Distributed Injection Attack Prevent Controller

In this part, we proposed a DETBC controller as

$$\Delta u_i(k)=\begin{cases}\varphi M_i(k)(x(\hat{\zeta}_i(k)-\zeta_i(k))-\hat{\zeta}_i(k)), & 0<k<T_3\\ \varphi M_{si}(k)(x(\hat{\zeta}_{si}(k)-\zeta_{si}(k))-\hat{\zeta}_{si}(k)), & T_3\le k\end{cases} \tag{33}$$

where $0<\varphi<1$, $M_i(k)=\hat{\Gamma}_i(k)/(\hat{\Gamma}_i^2(k)+\lambda)$, $0.5<x\le 1$, $\lambda>0$, and $M_{si}(k)=\hat{\Gamma}_{si}(k)/(\hat{\Gamma}_{si}^2(k)+\lambda)$. $\zeta_i(k)$ and $\zeta_{si}(k)$ are defined in Eqs. (2) and (11), respectively.

Theorem 4: If MASs (1) with Assumptions 1-5 is governed by the developed PPD estimation laws (12)-(13) and (16)-(17), the proposed RBFNN-based detection and compensation methods (10)-(11), and the formulated ET conditions (22)-(23) and (24)-(25), the proposed DETBC controller (33) can guarantee the MASs with bounded BC error $e_i(k)=s_iy_0(k)-y_i(k)$ to implement BC tasks under injection attack free or injection attack with Assumption 6.

Proof: **Case 1:** $0<k<T_3$. During this process, the controlled plant doesn't subject to the injection attack. From the ET conditions, it is concluded that if the BC error increases to exceed the conditions, the controlled plant will turn to the event-triggered process. Hence, we merely need to consider the convergence of the designed controller when $k=k_i$. In this case, $\breve{\zeta}_i(k)=\zeta_i(k)$ and $\Delta\breve{u}_i(k)=\Delta u_i(k)$. From Eqs. (18) and (33), we have

$$\begin{aligned}\hat{\zeta}_i(k+1) &= \hat{\zeta}_i(k) + x(\breve{\zeta}_i(k) - \hat{\zeta}_i(k)) \\ &\quad + \hat{\Gamma}_i(k)\varphi M_i(k)(x(\hat{\zeta}_i(k) - \zeta_i(k)) - \hat{\zeta}_i(k)) \\ &= (1-\hat{\Gamma}_i(k)\varphi M_i(k))\hat{\zeta}_i(k) \\ &\quad + (1-\hat{\Gamma}_i(k)\varphi M_i(k))xe_{\zeta i}(k)\end{aligned} \tag{34}$$

where $M_i(k) = \hat{\Gamma}_i(k)/(\hat{\Gamma}_i^2(k)+\lambda)$. Since $0<\varphi<1$, $\lambda>0$, there is a constant q_1 satisfying $0<|(1-\hat{\Gamma}_i(k)\varphi M_i(k))|<q_2<1$. Thus, according to $0.5<x\le 1$ and Eq. (34), we have

$$\begin{aligned}|\hat{\zeta}_i(k+1)| &\le q_2|\hat{\zeta}_i(k)| + q_2|e_{\zeta i}(k)| \\ &\le q_2|\hat{\zeta}_i(k)| + q_2 q_3 \\ &\cdots \\ &\le q_2^k|\hat{\zeta}_i(1)| + q_2 q_3(1-q_2^k)/(1-q_2)\end{aligned} \tag{35}$$

where $q_3 \ge |e_{\zeta i}(k)|$ since $e_{\zeta i}(k)$ is bounded. Hence, $\hat{\zeta}_i(k+1)$ is bounded. F. (2), we have $\zeta(k)=(L+B)e(k)$, where $\zeta(k)=[\zeta_1(k),\zeta_2(k),\cdots,\zeta_N(k)]^T$ and $e(k)=[e_1,e_2,\cdots,e_N]^T$. Hence, according to $e_{\zeta i}(k)=\zeta_i(k)-\hat{\zeta}_i(k)$ and Lemma 1, it is obtained that $e_i(k)$ is bounded.

Case 2: $T_3 \le k$. During this process, we can prove that $e_i(k)$ is also boundedusing the similar proof process of Case 1, therefore it is omitted. □

Remark 5: From the proof process, it is found that the definitional domain of the designed DETBC method's parameters, e.g. $0<\varphi<1$, $\lambda>0$, $0<h<1$, and $\theta>0$, don't rely on the communication topology and dynamics of MASs, that is, as increasing of the scale of MASs, we don't need to change the value of the parameters. However, the most existing data-driven distributed consensus methods [21], [38] require that the parameter φ of the controller must be less than the reciprocal of all diagonal entries $L+B$, and the topology $\bar{G}$ must be strongly connected.

Corollary 1: From the proof process in Theorem 4, it is easy to find that the form of $\zeta_i(k)$ doesn't affect the convergence of the proposed controller. Hence, the proposed method can be extended for leader-less BC control as

$$\zeta_i(k) = \sum_{j\in N_i} |a_{ij}|(sign(a_{ij})y_j(k) - y_i(k)) \tag{36}$$

for the bipartite containment control as

$$\begin{aligned}\zeta_i(k) &= \sum_{j\in N_i} |a_{ij}|(y_i(k) - sign(a_{ij})y_j(k)) \\ &\quad + \sum_{p=N+1}^{N+Z} b_{ip}(y_i(k) - s_i y_p(k))\end{aligned} \tag{37}$$

where Z is the number of leaders, $y_p(k)$ is the output of leader p, and $b_{ip}\in(0,1)$. If agent i is connected with the leader p, b_{ip}=1; otherwise b_{ip}=0.

Remark 6: From Eqs. (2), (36), and (37), the leader-follower consensus, leader-less consensus, and containment control are considered, where the number of the leaders and the communication topologies are different. It is noteworthy that the proposed fully distributed framework, DETBC, can be competent for the control as mentioned above requirements with the same parameters, where the topology restriction is further relieved than most existing approaches.

E. Extension to Switching Topologies

In this part, the time-varying switching topologies issue is investigated. Let $\bar{G}^l(k)$ denote all possible topologies of MASs, $l=1,2,\ldots,\kappa$, $\kappa\in Z^+$. Define $A^l(k)=[a_{ij}^l(k)]\in R^{N\times N}$, $D^l(k)=diag\{d_1^l(k),\cdots,d_N^l(k)\}$, $B^l(k)=diag\{b_1^l(k),\cdots,b_N^l(k)\}$, $L^l(k)$, and $s^l(k)=diag(s_1^l(k),\cdots,s_N^l(k))$ as the corresponding adjacency matrices, degree matrices, connecting matrices, Laplacian matrices, and grouping matrices, respectively.

Assumption 7: $\bar{G}^l(k)$ have a directed spanning tree, $l\in\kappa$.

Eq. (2) is modified as

$$\begin{aligned}\zeta_i(k) &= \sum_{j\in N_i} |a_{ij}^l(k)|(sign(a_{ij}^l(k))y_i(k) - y_j(k)) \\ &\quad + b_i^l(k)(s_i^l(k)y_0(k) - y_i(k))\end{aligned} \tag{38}$$

$$\begin{aligned}\zeta_{si}^l(k) &= \sum_{j\in N_i} |a_{ij}^l(k)|(sign(a_{ij}^l(k))y_{si}(k) - y_{sj}(k)) \\ &\quad + b_i^l(k)(s_i^l(k)y_0(k) - y_{si}(k) + \hat{f}_i^l(k))\end{aligned} \tag{39}$$

where $\hat{f}_i^l(k)$ is the output of RBFNN under the corresponding communication topology.

Theorem 5: If the MASs with Assumption 7 satisfies the restrictions and the control protocol of Theorem 4 and by only replacing Eqs. (2) and (11) using Eqs. (38) and (39), respectively, the BC error is bounded.

Proof: From Eqs. (2), (11), (38), and (39), it is easy to find that the proof process is the same as Theorem 4. Hence, this process is omitted.

IV. Simulation Study

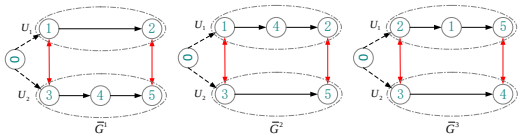

Fig. 3: The communication topologies of MASs

In this section, several simulation experiments are conducted to verify the correctness and effectiveness of the proposed DETBC scheme for the MASs with injection attacks. Figure 3 shows the communication topologies of MASs, where the information around the agents is transmitted along the arrow. The red arrow denotes the weight of this path is -1, otherwise, the weight is 1. The dynamics of agents with injection attack-free are

$y_1(k+1) = 0.5\cos(y_1(k)) + 0.7u_1(k)$,

$y_2(k+1) = y_2(k)u_2(k)/(1+y_2^3(k)) + 0.5u_2(k)$,

$y_3(k+1) = y_3(k)u_3^3(k)/(1+y_3^2(k)+u_3(k))$,

$y_4(k+1) = 0.7\sin(y_4(k)) + u_4(k)$,

$y_5(k+1) = 0.4\cos(y_5(k)) + 0.7u_5(k)$.

Let $y_{si}(k) = y_i(k) + f_{si}(k)$ with $i=1,2,3,4,5$ denote that the MASs are subject to injection attack or physical attack.

A. MASs with Fixed Topology

The graph $\bar{G}^1$ shown in Fig. 3 is selected as the communication topology for five heterogeneous agents. Firstly, to demonstrate the effectiveness of the proposed DETBC framework for three different control requirements, relavent results are presented in Fig. 4, where $f_{si}(k)$=0, $y_i(0)=u_i(k)=rand(-0.5,0.5)$ with $i=1,2,3,4,5$, φ=0.9, $\lambda=3.5$, h=0.9, θ=1, $u=0.01$, $\hat{r}=85$, and $x=1$.

For the leader-follower BC, the output of the leader is designed as $y_0(k)=1.5-(-0.5)^{round(k/3000)}$, and the running times is 10s. For containment control, the outputs of leaders are set as $y_5(k)=1.8\sin(k\Omega/1600)$ and $y_6(k)=0.8\cos(k\Omega/1600)$ with $0<k\le 5000$, $y_5(k)=0.5$ and $y_6(k)=2$ with $5000<k\le 10000$. The sample time is 0.001s. Moreover, the topology of containment control is selected as same with Fig. 1 in [39]. The corresponding results are presented in Fig 4, the designed DETBC can guarantee the MASs to implement different control tasks with good performances and smaller communication resources. From Figs. 4.d, 4.e, and 4.f, it is found that the designed RBFNN accurately predicts the output of each agent with different control protocols after a short online training process. From Figs. 4.h, 4.i, and 4.j, it is found that proposed DETBC only needs about 3.67%, 1.02%, and 0.36% communication resources to realize corresponding control tasks.

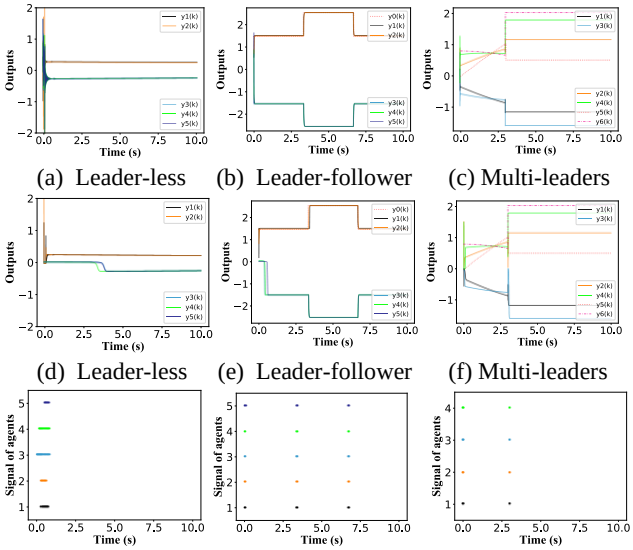

(a) Leader-less (b) Leader-follower (c) Multi-leaders

(d) Leader-less (e) Leader-follower (f) Multi-leaders

(h) Leader-less (i) Leader-follower (j) Multi-leaders

Fig. 4: Results of the designed DETBC method for MASs. (a), (b), and (c) are outputs of MASs. (d), (e), and (f) are corresponding predicted outputs of the established RBFNNs. (h), (i), and (k) are the corresponding ET signal of MASs.

As for the effectiveness of the designed RBFNN, several results for the MASs with time-varying reference being subject to injection attacks are shown in Fig. 5, where $f_1(k)=0.2\sin(2k\Omega/50)$, $f_2(k)=0.3\sin(2k\Omega/40)$, $f_3(k)=0.3\cos(2k\Omega/40)$, $f_4(k)=0.3\cos(k\Omega/30)+0.2\sin(k\Omega/40)$, $f_5(k)=0.3\sin(k\Omega/50)$, and $y_0(k)=0.3\cos(k\Omega/2000)+0.5\sin(k\Omega/6000)+1$.

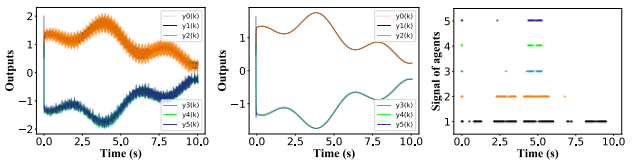

(a) without RBFNN (b) with RBFNN (c) Triggering signal

Fig. 5: Results of the designed DETBC method for MASs with injection attack.

Figure 5 shows that the designed RBFNN is also fitting the time-varying tracking tasks, which further verifies the correctness and effectiveness of Theorems 1-4.

B. MASs with Switching Topologies

The time-varying switching topologies problem is investigated, which are changed as $\bar{G}^i=\bar{G}^1$, $0<k\le 3000$; $\bar{G}^i=\bar{G}^2$, $3000<k\le 6000$; $\bar{G}^i=\bar{G}^3$, $6000<k\le 10000$. The results are presented in Fig. 6, where $y_0(k)=0.5\sin(k\Omega/6000)+0.7$. Other parameters are set the same as Section IV.A. From Fig. 6, we can see that the designed DETBC can also govern the MASs with injection attacks and switching topologies to implement BC tracking tasks, which demonstrates the correctness of Theorem 5.

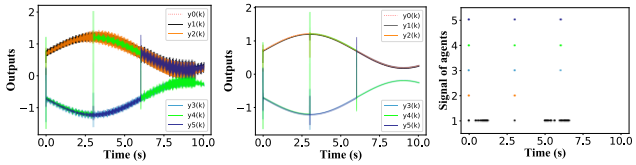

(a) without RBFNN (b) with RBFNN (c) Triggering signal

Fig. 6: Results of the designed DETBC method for MASs with switching topologies and injection attacks.

V. Hardware Tests

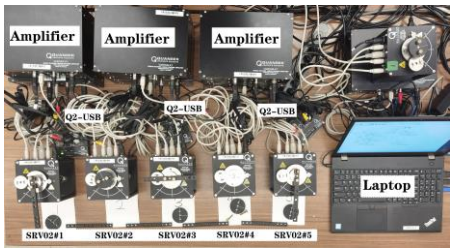

Fig. 7: The hardware system with SRV02 units.

In this Section, some hardware test results are presented, where five heterogeneous SRV02 units of Quanser are employed to establish the hardware platform. Moreover, the hardware system also includes five amplifiers and three Q2-USB data acquisitions shown in Fig. 7. It noted that the value of parameters and simple time are set the same as Section V.A. The desired speed is set as $y_0(k)=2+(-1)^{round(k/3000)}$.

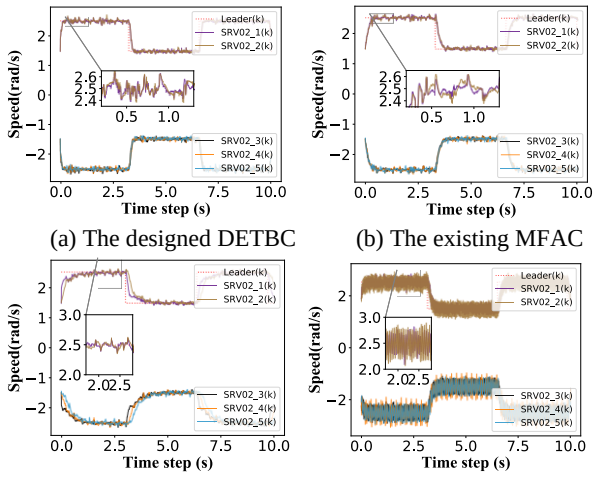

(a) The designed DETBC (b) The existing MFAC

(c) The designed DETBC (d) The existing MFAC

Fig. 8: The output of bipartite consensus with five SRV02: (a) and (b) are outputs of the SRV02 with injection attack free. (c) and (d) are the outputs of the SRV02 with injection attack.

Compared with Figs. 8.a and 8.b, it is found that the proposed DETBC has a better convergence rate than prior MFAC in [21]. Meanwhile, from Figs. 8.c and 8.d, we can

find that DETBC can effectively reduce the effects of injection attacks. Moreover, the average ET times of 8.a and 8.c are 3592.4 and 5451.8, respectively, where the total number of samples is 10^4. In other words, the designed DETBC can save nearly 95% of communication resources than the existing method. It further verifies the effectiveness and practicality of the designed method.

VI. Conclusions

An enhanced compact form dynamic linearization model has been established. A fully distributed event-triggered bipartite consensus framework has been formulated for nonlinear nonaffine discrete-time MASs with fixed and switching topologies. Moreover, RBFNN-based detection and compensation schemes for injection attacks have been proposed. Compared with most existing data-driven methods, the proposed schemes improve the convergence rate and applicability , relieve the communication burden sharply, and reduce the restriction of the topology of MASs. The extendion of the proposed schemes for the multi-input multi-output MASs is meaningful in our future works.

Appendix A
Proof of Theorem 1

Let $Y_i(k)=\Xi_i(k)-P_i(y_i(k-1),u_i(k-1),y_j(k-1),u_j(k-1))$, and $\Xi_i(k)=P_i(y_i(k),u_i(k-1),y_j(k),u_j(k))$. From Eq. (4), we have

$$\Delta\boldsymbol{\zeta}_i(k+1)=P_i(y_i(k),u_i(k),y_j(k),u_j(k))-\Xi_i(k)+Y_i(k) \quad (40)$$

Using differential mean value theorem and Assumptions 1 and 2, we have

$$\Delta\boldsymbol{\zeta}_i(k+1)=\partial P_i^*/\partial u_i(k)+Y_i(k) \quad (41)$$

Applying $|\Delta u_i(k)|>\delta$ defined in Eq. (13) and Assumption 3 for all k , there is $G_i^*(k)$ satisfying $Y_i(k)=G_i^*(k)\Delta u_i(k)$. Then, let $\Gamma_i(k)=\partial P_i^*/\partial u_i(k)+G_i^*(k)$, and from Eq. (41), the following equation is obtained

$$\Delta\boldsymbol{\zeta}_i(k+1)=\Gamma_i(k)\Delta u_i(k) \quad (42)$$

Taking absolute from both sides of $\Delta\boldsymbol{\zeta}_i(k+1)$, and using Assumptions 2 and 3, and Eq. (2), it is obtained that

$$\begin{aligned}|\Delta\boldsymbol{\zeta}_i(k+1)|=&|\sum_{j\in N_i}|a_{ij}|(sign(a_{ij})\Delta y_i(k+1)-\Delta y_j(k+1))\\&+b_i(s_i\Delta y_0(k+1)-\Delta y_i(k+1))|\\\le&|\sum_{j\in N_i}|a_{ij}|(sign(a_{ij})r|\Delta u_i(k)|+rr_\Delta|\Delta u_i(k)|)\\&+b_i(s_ir_0+r|\Delta u_i(k)|)|\\\le&|\sum_{j\in N_i}|a_{ij}|(sign(a_{ij})r|\Delta u_i(k)|+rr_\Delta|\Delta u_i(k)|)|\\&+b_ir|\Delta u_i(k)|+\bar{G}|\Delta u_i(k)|\\\le&(N(1+r_\Delta)r+b_ir+\bar{G})|\Delta u_i(k)|\\\le&r_{\boldsymbol{\zeta}}|\Delta u_i(k)|\end{aligned} \quad (43)$$

where $r_{\boldsymbol{\zeta}}=(N(1+r_\Delta)r+r+\bar{G})$ and $r_0/r_u\le\bar{G}\le r_0/\boldsymbol{\delta}$. Hence, from Eqs. (42) and (43), we have $\Gamma_i(k)\le r_{\boldsymbol{\zeta}}$.

References

[1] Li Y, Tan C. A survey of the consensus for multi-agent systems[J]. Systems Science & Control Engineering, 2019, 7(1): 468-482.

[2] Zhang D, Feng G, Shi Y, et al. Physical safety and cyber security analysis of multi-agent systems: A survey of recent advances[J]. IEEE/CAA Journal of Automatica Sinica, 2021, 8(2): 319-333.

[3] Mei J, Ren W, Song Y. A Unified Framework for Adaptive Leaderless Consensus of Uncertain Multi-agent Systems under Directed Graphs[J]. IEEE Transactions on Automatic Control, 2021.

[4] Chen C, Lewis F L, Li X. Event-triggered coordination of multi-agent systems via a Lyapunov-based approach for leaderless consensus[J]. Automatica, 2021: 109936.

[5] Zegers F, Deptula P, Shea J M, et al. Event/Self-Triggered Approximate Leader-Follower Consensus with Resilience to Byzantine Adversaries[J]. IEEE Transactions on Automatic Control, 2021.

[6] Li H, Liu Q, Feng G, et al. Leader–follower consensus of nonlinear time-delay multiagent systems: A time-varying gain approach[J]. Automatica, 2021, 126: 109444.

[7] Movric K H, Lewis F L. Cooperative optimal control for multi-agent systems on directed graph topologies[J]. IEEE Transactions on Automatic Control, 2013, 59(3): 769-774.

[8] Li Z, Wen G, Duan Z, et al. Designing fully distributed consensus protocols for linear multi-agent systems with directed graphs[J]. IEEE Transactions on Automatic Control, 2014, 60(4): 1152-1157.

[9] Lv Y, Li Z. Is fully distributed adaptive protocol applicable to graphs containing a directed spanning tree?[J]. Science China Information Sciences, 2022, 65(8): 1-2.

[10] Wang H, Ren W, Yu W, et al. Fully distributed consensus control for a class of disturbed second-order multi-agent systems with directed networks[J]. Automatica, 2021, 132: 109816.

[11] Zhang Z, Chen S M, Zheng Y. Fully Distributed Scaled Consensus Tracking of High-order Multi-agent Systems with Time Delays and Disturbances[J]. IEEE Transactions on Industrial Informatics, 2021.

[12] Jiang H, He H. Data-driven distributed output consensus control for partially observable multiagent systems[J]. IEEE transactions on cybernetics, 2018, 49(3): 848-858.

[13] Li H, Wu Y, Chen M, et al. Adaptive multigradient recursive reinforcement learning event-triggered tracking control for multiagent systems[J]. IEEE Transactions on Neural Networks and Learning Systems, 2021.

[14] Hou Z, Jin S. A novel data-driven control approach for a class of discrete-time nonlinear systems[J]. IEEE Transactions on Control Systems Technology, 2010, 19(6): 1549-1558.

[15] Lin N, Chi R, Huang B. Event-triggered model-free adaptive control[J]. IEEE Transactions on Systems, Man, and Cybernetics: Systems, 2019.

[16] Liu D, Yang G H. Neural network-based event-triggered MFAC for nonlinear discrete-time processes[J]. Neurocomputing, 2018, 272: 356-364.

[17] Wang Z, Liu L, Zhang H. Neural network-based model-free adaptive fault-tolerant control for discrete-time nonlinear systems with sensor fault[J]. IEEE Transactions on Systems, Man, and Cybernetics: Systems, 2017, 47(8): 2351-2362.

[18] Wang Y, Wang Z. Data-Driven Model-Free Adaptive Fault-Tolerant Control for a Class of Discrete-Time Systems[J]. IEEE Transactions on Circuits and Systems II: Express Briefs, 2021.

[19] Qiu X, Wang Y, Xie X, et al. Resilient model-free adaptive control for cyber-physical systems against jamming attack[J]. Neurocomputing, 2020, 413: 422-430.
[20] Yu W, Wang R, Bu X, et al. Resilient Model-Free Adaptive Iterative Learning Control for Nonlinear Systems Under Periodic DoS Attacks via a Fading Channel[J]. IEEE Transactions on Systems, Man, and Cybernetics: Systems, 2021.
[21] Bu X, Hou Z, Zhang H. Data-driven multiagent systems consensus tracking using model free adaptive control[J]. IEEE transactions on neural networks and learning systems, 2017, 29(5): 1514-1524.
[22] Xiong S, Hou Z. Data-Driven Formation Control for Unknown MIMO Nonlinear Discrete-Time Multi-Agent Systems With Sensor Fault[J]. IEEE Transactions on Neural Networks and Learning Systems, 2021.
[23] Ma Y S, Che W W, Deng C, et al. Distributed Model-Free Adaptive Control for Learning Nonlinear MASs Under DoS Attacks[J]. IEEE Transactions on Neural Networks and Learning Systems, 2021.
[24] Dimarogonas D V, Frazzoli E, Johansson K H. Distributed event-triggered control for multi-agent systems[J]. IEEE Transactions on Automatic Control, 2011, 57(5): 1291-1297.
[25] Zhang J, Zhang H, Sun S, et al. Leader-follower consensus control for linear multi-agent systems by fully distributed edge-event-triggered adaptive strategies[J]. Information Sciences, 2021, 555: 314-338.
[26] Sun H J, Xia R, Yu A. Fully Distributed Event-Triggered Consensus for a Class of Second-Order Nonlinear Multi-agent Systems[J]. Circuits, Systems, and Signal Processing, 2021: 1-18.
[27] Li W, Zhang H, Wang W, et al. Fully distributed event-triggered time-varying formation control of multi-agent systems subject to mode-switching denial-of-service attacks[J]. Applied Mathematics and Computation, 2022, 414: 126645.
[28] Mu X, Gu Z, Hua L. Memory-based event-triggered leader-following consensus for TS fuzzy multi-agent systems subject to deception attacks[J]. Journal of the Franklin Institute, 2021.
[29] Li X M, Zhou Q, Li P, et al. Event-triggered consensus control for multi-agent systems against false data-injection attacks[J]. IEEE transactions on cybernetics, 2019, 50(5): 1856-1866.
[30] Ahmed Z, Saeed M A, Jenabzadeh A, et al. Frequency domain analysis of resilient consensus in multi-agent systems subject to an integrity attack[J]. ISA transactions, 2021, 111: 156-170.
[31] Dong H, Li C, Zhang Y. Resilient consensus of multi-agent systems against malicious data injections[J]. Journal of the Franklin Institute, 2020, 357(4): 2217-2231.
[32] Altafini C. Consensus problems on networks with antagonistic interactions[J]. IEEE transactions on automatic control, 2012, 58(4): 935-946.
[33] Chen Y, Zuo Z, Wang Y. Bipartite consensus for a network of wave PDEs over a signed directed graph[J]. Automatica, 2021, 129: 109640.
[34] Sakthivel R, Parivallal A, Manickavalli S, et al. Resilient dynamic output feedback control for bipartite consensus of multiagent systems with Markov switching topologies[J]. International Journal of Robust and Nonlinear Control, 2021.
[35] Peng Z, Hu J, Shi K, et al. A novel optimal bipartite consensus control scheme for unknown multi-agent systems via model-free reinforcement learning[J]. Applied Mathematics and Computation, 2020, 369: 124821.
[36] Park J, Sandberg I W. Universal approximation using radial-basis-function networks[J]. Neural computation, 1991, 3(2): 246-257.
[37] Yu Q, Hou Z, Bu X, et al. RBFNN-based data-driven predictive iterative learning control for nonaffine nonlinear systems[J]. IEEE transactions on neural networks and learning systems, 2019, 31(4): 1170-1182.
[38] Yu X, Hou Z, Polycarpou M M. Distributed Data-Driven Iterative Learning Consensus Tracking for Nonlinear Discrete-Time Multi-Agent Systems[J]. IEEE Transactions on Automatic Control, 2021.
[39] Zhang H, Zhou Y, Liu Y, et al. Cooperative bipartite containment control for multiagent systems based on adaptive distributed observer[J]. IEEE Transactions on Cybernetics, 2020.